Russian Journal of Biomechanics
www.biomech.ac.ru

MODELS OF MICROCIRCULATION AND EXTRAVASCULAR FLUID EXCHANGE

Y.I. Nyashin, M.Y. Nyashin, N.S. Shabrykina

Department of Theoretical Mechanics, Perm State Technical University, 29a, Komsomolskii Prospect, 614600, Perm, Russia, e-mail: sns@theormech.pstu.ac.ru

Abstract. Circulatory and lymphatic systems deliver nutrients to organs and tissues of the human or animal body and the removal of wastes to the excretory system. The exchange of fluid, containing nutrients or metabolic products, takes place at the microcirculation level and consists of the following interrelated processes: blood flow in capillaries, transvascular exchange, fluid movement in the interstitium, exchange between interstitial fluid and tissue cells and lymphatic drainage. Filtration and diffusion are the main driving forces for the substances exchange. The present paper is a review of mathematical models dealing with exchange processes.

Key words: microcirculation, transcapillary fluid exchange, mathematical modeling

Introduction

The delivery of nutrients to, and removal of metabolic products from the cells of the body is an important problem that all large organisms must solve. This task can be divided into two major steps. The first one is the macroscale circulation of the blood through the arteries and veins of the body, responsible for transporting large quantities of substances among the various organs and systems. Oxygen from the lungs and food from the gut are delivered to the rest of the body, and wastes are brought to the liver and kidneys. This process is almost purely convective. The second step is the microscale exchange of substances between the capillaries and living cells of the surrounding tissue. Although convection is important in the microcirculation, the spatial scales are small enough that molecular diffusion is also a significant process.

Microcirculatory transport is governed by the structure of the capillary wall and interstitial matrix. Changes in these components play an important role in the development and progression of several diseases. Abnormally high capillary permeability developing with advanced diabetes and cardiac edema induced by heart failure, and the loss of proteoglycans and glycosaminoglycans from the extracellular matrix lead to the development of osteoarthritis. Changes in vascular permeability and interstitial matrix characteristics play a dominant role in the physiological response to a burn injury. Microcirculatory phenomena affect the delivery of drugs to a disease site. Additionally, the ability to generate normal mass transport characteristics in artificial tissues is crucial for creating usable products.

Modern ideas about the nature of exchange between the circulatory and extravascular body fluids date back to the Starling's hypothesis [17] that the flux of water across the capillary wall is determined by opposing hydrostatic and osmotic pressures. According to the Starling's hypothesis, the capillary wall is a passive barrier to fluid exchange and the system

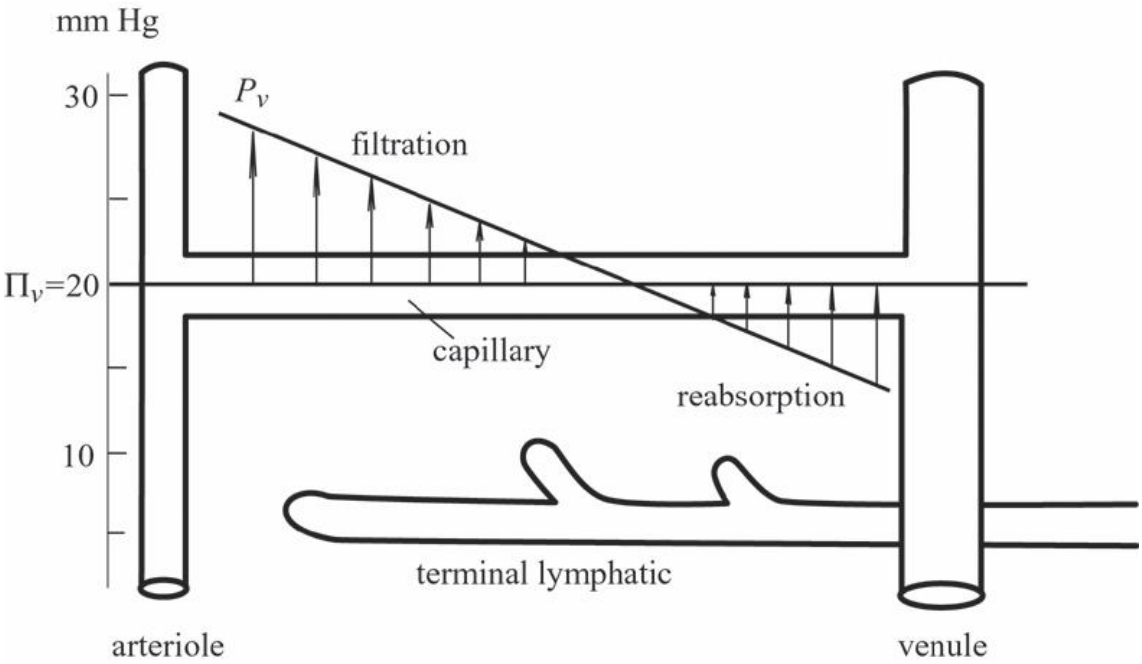

Fig. 1. A typical capillary: an illustration for the Starling's hypothesis.

will reach equilibrium when the hydrostatic pressure difference between the capillary and interstitium is balanced by the opposing osmotic pressure difference.

The next equation describes the Starling's hypothesis:

$$J_v = L_p S\left(\left(P_v - P_i\right) - \left(\Pi_v - \Pi_i\right)\right) = L_p S\left(\Delta P - \Delta\Pi\right), \quad (1)$$

where J_v is the transcapillary volume flux, P_v and P_i are the capillary and interstitial fluid hydrostatic pressures, Π_i and Π_v are the interstitial fluid and blood plasma colloid osmotic pressures, L_p is the hydraulic conductivity of the capillary wall and S is the surface area available for exchange.

When the value J_v is positive, the fluid filtrates from the capillary; when J_v is negative, reabsorption takes place: fluid moves from the tissue back into the capillary. Starling believed that the hydrostatic interstitial pressure P_i is equal to the interstitial colloid osmotic pressure Π_i. Thus filtration occurs at the arterial end of the capillary where the hydrostatic pressure is high and reabsorption occurs at the venous end where the pressure is low (Fig. 1). Also there is a spot in the capillary where there is neither filtration nor reabsorption due to equality of filtration and reabsorption driving forces. Besides Starling thought that under normal conditions filtration slightly exceeds reabsorption so a part of the fluid stays in the tissue and drainages into the lymphatic system afterwards.

Investigations performed by Landis [11, 12] and Pappenheimer [13] gave the Starling's hypothesis an experimental basis.

Starling's ideas were developed more fully when Kedem and Katchalsky [9] used the ideas of nonequlibrum thermodynamics to derive equations for mass transport across membranes. The transport of solute and water across a membrane was now understood to be a process coupled by osmotic effects.

Kedem and Katchalsky equations give volume and solute fluxes and can be written in the following form:

$$J_v = L_p S\left(\Delta P - \sigma_T \Delta\Pi\right), \quad (2)$$

$$J_s = pS\Delta C + J_v\left(1-\sigma_T\right)\tilde{C}, \quad (3)$$

where J_s is the solute flux, $\Delta C = C_v - C_i$ is the difference of solute concentration between vascular and interstitial fluids, $\tilde{C}$ is the logarithmic mean of solute concentration on either side of the capillary wall and p is the wall permeability.

The first equation is identical to the Starling's equation, with the addition of the factor σ_T, the solute reflection coefficient. This parameter varies between 0 for a freely permeable solute and 1 for an impermeable solute, and is a measure of the relative selectivity of the membrane for the solute compared to the bulk solution.

By the late 1950s it was understood that transcapillary exchange of water and solutes is governed by the differences in two driving forces on either side of the capillary wall: hydrostatic pressure and concentration gradient. From then on the development of mathematical models describing blood microcirculation in conjunction with transcapillary exchange, interstitial movement and lymphatic drainage was started. This paper presents a review of such models.

Fluid movement in a microvessel with permeable walls surrounded by porous medium

In this section models of fluid movement in a blood microvessel surrounded by porous medium are presented. Such models describe flow of both blood plasma (considered as a Newtonian fluid) and whole blood (considered as different types of non-Newtonian fluid). Boundary conditions on the vessel-tissue boundary are also different. Fluid movement in porous medium (tissue) is described by the Darcy's law.

It is usually assumed that all capillaries in an organ are similar with respect to dimensions, blood flow characteristics, etc. Thus only a single representative capillary needs to be modeled. The single capillary model introduced in 1919 by Krogh is the simplest one of this kind. The model consists of a straight capillary and a concentrically surrounding tissue mantle (Fig. 2). At R_G the medium becomes impermeable and rigid. The system therefore has a constant volume and cannot accumulate fluid. This condition means that there is no fluid exchange between neighbouring capillary regions.

In [1] the slow flow of the blood plasma as a Newtonian incompressible fluid is examined. The complete set of equations (Navier-Stokes) governing fluid flow in the capillary is:

$$\begin{aligned} &\frac{\partial \boldsymbol{U}}{\partial t} + (\boldsymbol{U}\cdot\nabla)\boldsymbol{U} = \boldsymbol{F} - \frac{1}{\rho}\nabla P + \nu\nabla^2\boldsymbol{U}, \\ &div\,\boldsymbol{U} = 0, \end{aligned} \tag{4}$$

where $\boldsymbol{U}$ is the velocity vector, ν is the kinematic viscosity, ρ is the fluid density, P is the fluid pressure and $\boldsymbol{F}$ are the external forces.

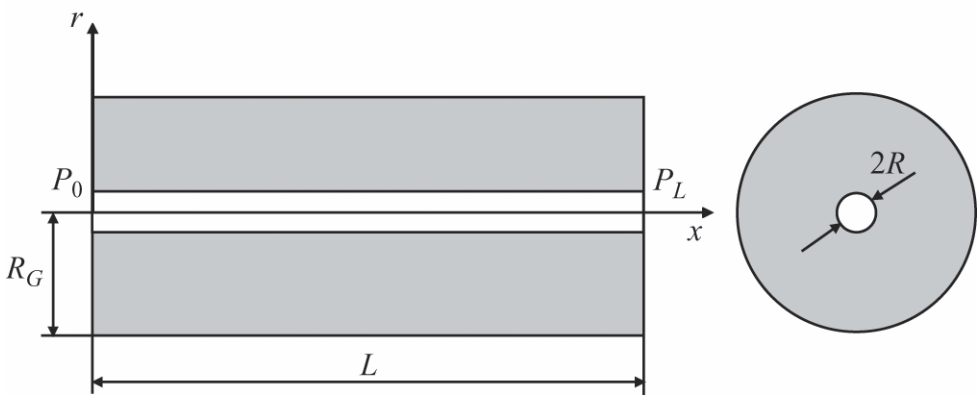

Fig. 2. A capillary surrounded by tissue (the Krogh's model).

Since the flow is laminar equations (4) take the form:

$$\frac{\partial P}{\partial x} = \eta\left(\frac{\partial^2 u}{\partial r^2} + \frac{1}{r}\frac{\partial u}{\partial r}\right), \quad 0 \le x \le L,$$
$$\frac{\partial P}{\partial r} = 0 \text{ or } P = P(x), \tag{5}$$
$$\frac{\partial u}{\partial x} + \frac{\partial v}{\partial r} + \frac{v}{r} = 0.$$

In the above, u and v are the axial and radial components of the velocity, respectively, $\boldsymbol{U} = (u;v) = (u(x,r);v(x,r))$ and η is the viscosity.

The tissue region is treated as an isotropic porous medium where the Darcy's law is applicable:

$$\boldsymbol{U} = -\frac{K}{\eta}\nabla P\,. \tag{6}$$

The velocity vector is average over a tissue volume that is large compared with the volume of individual pore. K is the Darcy's constant characterizing the porosity of the medium.

The equations of motion and the continuity equation for the tissue region are:

$$\bar{u}(x,r) = -\frac{K}{\eta}\frac{\partial \bar{P}}{\partial x},$$
$$\bar{v}(x,r) = -\frac{K}{\eta}\frac{\partial \bar{P}}{\partial r}, \tag{7}$$
$$\frac{\partial^2 \bar{P}}{\partial r^2} + \frac{1}{r}\frac{\partial \bar{P}}{\partial r} + \frac{\partial^2 \bar{P}}{\partial x^2} = 0.$$

The quantities in the tissue region are denoted by superscript bar.

The boundary conditions of the problem are:

$$\begin{aligned} &P(0,r) = P_0,\\ &P(L,r) = P_L,\\ &u(x,R) = 0,\\ &P(x,R) = \bar{P}(x,R),\\ &v(x,R) = \bar{v}(x,R),\\ &\bar{v}(x,R_G) = 0,\\ &\bar{u}(0,r) = 0,\\ &\bar{u}(L,r) = 0. \end{aligned} \tag{8}$$

It means that the non-slip conditions are applied to solve the problem. The last three equations express the fact that tissue is surrounded by an impervious cylinder.

Equations (5), (7) with boundary conditions (8) have an analytical solution. Solution analysis for physiological parameters of the basic functional unit shows that the flow in the capillary with low wall permeability is very close to the Poiseuille's flow. Therefore the solution is:

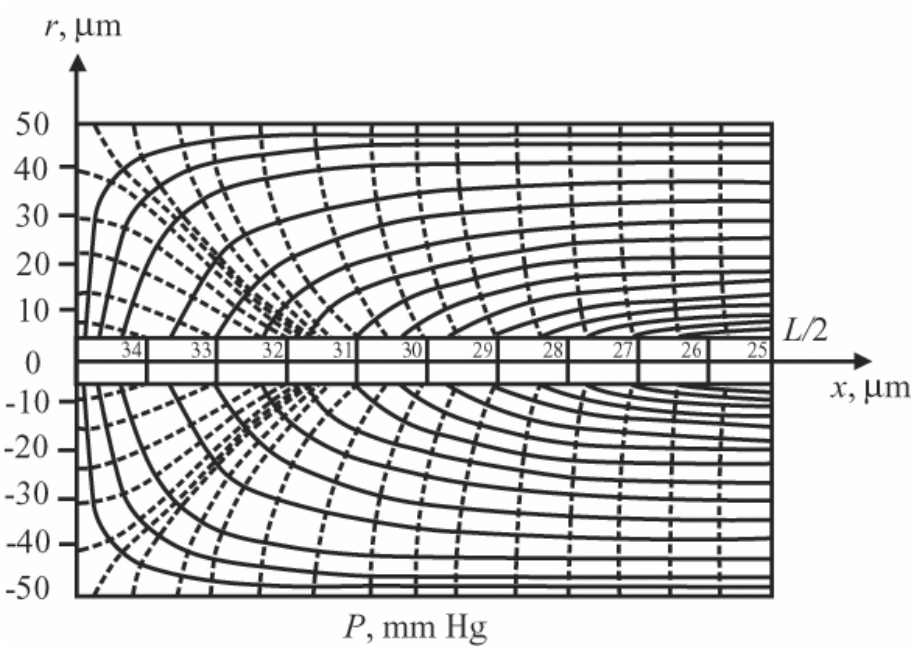

Fig. 3. Distribution of pressure (dashed lines) and streamlines (solid lines) in the tissue surrounding the capillary, $L = 300\ ?\text{m}$, $K = 10^{-14}\ \text{cm}^2$.

$$u(x,r) = \frac{P_0 - P_L}{4\eta L}\left(R^2 - r^2\right),$$

$$P(x) = P_0 + \left(P_0 - P_L\right)\frac{x}{L}, \qquad (9)$$

$$Q_u = -\frac{\pi R^4}{8\eta}\frac{P_0 - P_L}{L},$$

where Q_u is the total amount of fluid entering the basic functional unit per unit time - the total flow rate. Equations (9) give a parabolic velocity profile and a linear pressure distribution along the capillary.

Distribution of pressure and streamlines in the tissue around the capillary are given in Fig. 3. Only the arterial (i.e. high pressure) half of the unit is shown. Filtration takes place mostly near the arterial end of the capillary. The tissue is mostly under an axial pressure gradient, which is close to the pressure gradient in the capillary, and the flow is for the most part parallel to the capillary axis.

Fluid flow in an artery with an occlusion or stenosis is studied in [16]. The fluid is also assumed to be Newtonian but at the vessel-tissue boundary the condition proposed by Beavers and Joseph [8] is used:

$$\dot{\gamma}_{rx} = \frac{\alpha}{\sqrt{K}}\left(u_B - Q\right), \qquad (10)$$

where $\dot{\gamma}$ is the rate of strain tensor, u_B is the mean velocity parallel to the surface, α is the slip parameter depending only on the medium properties and Q is the tangential volume flow rate at the boundary. Beavers and Joseph proposed this condition empirically and then it was confirmed by different experiments.

If the wall slope is everywhere negligible (as for the narrow capillary), equations (5) with the boundary condition (10) produce the following solution:

$$
\begin{aligned}
u &= \frac{Q_u}{2R} + \frac{\alpha\sigma}{4R^3}\left(\frac{Q_u - 2RQ}{3+\alpha\sigma}\right)\left(R^2 - 3r^2\right), \\
v &= 0, \\
Q_u &= -\frac{2R^3}{3\eta}\left(\frac{3\alpha + \sigma\left(3+\alpha\sigma\right)}{\alpha\sigma^2}\right)\frac{\partial P}{\partial x}, \\
\frac{\partial P}{\partial r} &= 0, \\
P &= \frac{3\alpha\eta}{2}\int_c^x \frac{\sigma\left(2RQ - Q_u\right)}{R^3\left(3+\alpha\sigma\right)}dx,
\end{aligned}
\tag{11}
$$

where c is a constant of integration.

A Newtonian fluid was under consideration in above presented models. But for the blood flowing in microvessels this supposition cannot be applied since the size of blood cells is comparable with the size of a capillary. Therefore such models can describe only the flow of the blood plasma. In what follows we will discuss the flow of non-Newtonian fluid.

The Casson constitutive equation has been used many times to simulate the rheological properties of the blood flowing in small tubes since the original suggestion in 1959, and for a number of years it was considered to be the most accurate law. In such a way Das and Batra [4] applied the Casson's equation to describe the blood flow in the form:

$$\sqrt{\tau} = \sqrt{\tau_y} + k_c\sqrt{\dot{\gamma}}\,, \tag{12}$$

where τ represents the shear stress, k_c^2 is the Casson viscosity, $\dot{\gamma}$ is the rate of strain component and τ_y is the yield value, which for blood is related to the hematocrit by the relation $\sqrt[3]{\tau_y} = \dfrac{a\left(Ht - Ht_m\right)}{100}$. Here Ht is the normal hematocrit, Ht_m is the hematocrit below which there is no yield stress, and $a = 0.0037 \pm 0.001\sqrt[3]{\mathrm{H/m}^2}$.

Under given conditions the basic equation governing the flow

$$\frac{1}{r}\frac{\partial}{\partial r}\left(r\tau_{rx}\right) = -\frac{dP}{dx}, \tag{13}$$

has the following solution:

$$\tau_{rx} = -\frac{r}{2}\frac{dP}{dx}, \tag{14}$$

under the condition that τ_{rx} is finite at $r = 0$.

Casson fluid possesses a yield value, so in the regions where shear stress is less than the yield value, there will be no flow and the material will move as a whole with a constant velocity, giving rise to a symmetrical plug core formation around the axis (Fig. 4). If u_C is the velocity of the core and R_C is its radius, the following conditions are satisfied:

$$\frac{du}{dr} = 0, \quad u = u_C \text{ at } r = R_C\,. \tag{15}$$

Relation (12) can be written in terms of the velocity gradient as follows:

$$
\begin{cases}
\dfrac{\partial u}{\partial r} = -f(\tau) = -\left(\dfrac{\sqrt{\tau_{rx}} - \sqrt{\tau_y}}{k_c}\right)^2, & |\tau| \ge \tau_y, \\
\dfrac{\partial u}{\partial r} = f(\tau) = 0, & |\tau| < \tau_y.
\end{cases}
\tag{16}
$$

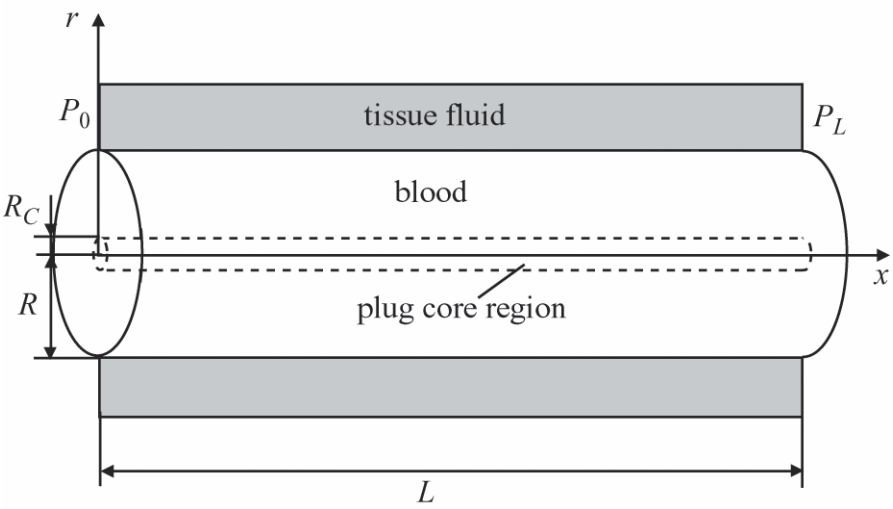

Fig. 4. Casson's fluid in the capillary.

Now substituting the expression (14) into (16) we get the differential equation in the flow region:

$$-\frac{\partial u}{\partial r}=\frac{1}{k_c^2}\left(\frac{r}{2}\sqrt{\left|\frac{dP}{dx}\right|}-\sqrt{\tau_y}\right)^2. \tag{17}$$

The above equation is to be solved under the slip condition at the wall:

$$u\big|_{r=R}=u_B, \tag{18}$$

where the slip velocity u_B satisfies the relation

$$\left.\frac{\partial u}{\partial r}\right|_{r=R}=\frac{\alpha}{\sqrt{K}}\left(u_B-Q\right). \tag{19}$$

Here Q is the velocity in the porous region given by:

$$Q=-\frac{K}{k_c^2}\frac{dP}{dx}. \tag{20}$$

Relation (19) is the modified Beavers and Joseph condition for porous medium.

The volumetric flow rate can be defined as:

$$Q_u=2\pi\int_0^R urdr=\frac{\pi R^3}{\tau_R^3}\int_0^{\tau_R}\tau_{rx}^2 f(\tau)d\tau+\pi R^2 u_B, \tag{21}$$

where $\tau_R=\tau_{rx}\big|_{r=R}$ is the wall shear stress.

Another model of a non-Newtonian fluid flow is presented in the paper [19]. Authors consider the flow of Bingham fluid through a circular pipe with a permeable wall. For the flow we have Eq. (13) with the solution (14). Substituting the last expression in

$$\tau_{rx}=-\eta\frac{du}{dr}+\tau_C,$$

we get

$$\tau_C-\eta\frac{du}{dr}=-\frac{r}{2}\frac{dP}{dx}, \tag{22}$$

where $\tau_C=\tau\big|_{r=R_C}$.

The boundary conditions are Beavers and Joseph conditions (18), (19), where $Q = \frac{p}{\sigma^2}$ and $\sigma = \frac{R}{\sqrt{K}}$ is dimensionless parameter.

The solution of the problem is:

$$
\begin{aligned}
u &= -\frac{R^2}{4\eta}\frac{dP}{dx}\left(1-\frac{r^2}{R}\right)-\frac{\tau_C R}{\eta}\left(1-\frac{r}{R}\right)+u_B, \text{ where } r \ge r_C,\\
u_C &= -\frac{R^2}{4\eta}\frac{dP}{dx}\left(1-\frac{r_C}{R}\right)+u_B, \text{ where } r \le r_C,\\
u_B &= \frac{\sqrt{K}}{\eta}\frac{dP}{dx}\left(\frac{R}{2\alpha}-\sqrt{K}\right)+\frac{\sqrt{K}}{\alpha}\frac{\tau_C}{\eta},\\
Q_u &= -\frac{\pi}{8\eta}\frac{dP}{dx}R^4\left(1-\frac{4}{3}\frac{\tau_C}{\tau_R}+\frac{1}{3}\left(\frac{\tau_C}{\tau_R}\right)^4\right)+\pi R^2 u_B.
\end{aligned}
\qquad (23)
$$

Hogan and Henriksen [5] use micropolar extension of continuum mechanics to describe flow of the blood in small arteries. The distinguishing feature of the micropolar theory is the introduction of a particle rotation that is independent of the classical rotation of the surrounding fluid. The existence of particle microrotation gives rise to couple stresses in addition to traditional tractional stresses. The analysis indicates that results obtained using a micropolar fluid model differ substantionally from those obtained with a classical Newtonian formulation. Thus, the question of whether a micropolar fluid is indeed a more accurate model for the whole blood remains opened. The proper boundary conditions for microspin are an unresolved issue too.

There are many kinds of blood constitutive equations other than considered ones. They can be categorized as Casson type (Casson equation, Luo and Kuang equation, Quemada equation, Cross equation, Wang equation) and power-law type (power law equation, Weaver equation, Walburn equation) because they can be obtained by developing the Casson equation and the power-law equation, respectively. Comparison with experimental data proves Luo and Kuang equation and Quemada equation to be the best models for the blood flow in a capillary [15, 21].

All presented models describe the blood flow in a capillary and surrounding tissue under the hydrostatic pressure gradient. Using different constitutive equations and boundary conditions these models give pressure and velocity distribution in the capillary and surrounding tissue. But none of these models consider the influence of diffusion on extracapillary fluid exchange or lymphatic drainage. These factors are taken into consideration in what follows.

Dynamics of fluid movement between intravascular and interstitial spaces

Isogai et al. [6] investigated dynamics of fluid movement between intravascular and interstitial spaces. Infusion of the Ringer's solution or transfusion of the whole blood into the intravascular space causes change in blood and plasma colloid osmotic pressures and induces a fluid redistribution between the intravascular and interstitial spaces. The redistribution results from a loss of equilibrium of the effective filtration pressure of water on the capillary wall.

Fluid injected into the intravascular space changes the blood and colloid osmotic pressures, if the colloid osmotic pressure of the injected fluid differs from that of the blood.

Changes in these two pressures, in turn, alter the effective filtration pressure across the capillary wall and generate flows of water and proteins. The flows of water and proteins affect the volume and the colloid osmotic pressure of the intravascular and interstitial fluids. The changes of the volume and the colloid osmotic pressure of fluids in both of the spaces modify the effective filtration pressure across the capillary wall and affect the flow of the fluid across it in a recurrent dynamic fashion.

The system under consideration is visualized as being composed of two tanks; one represents the intravascular space and the other represents the interstitial space. The two tanks are connected by a pipe through which fluid and proteins can exchange. The pipe represents the capillary wall. The intravascular and the interstitial spaces volumes are V_v and V_i, respectively. A tank of the intravascular space has a faucet through which the infused fluid of the hematocrit value Ht flows into the space with the rate J.

Kedem and Katchalsky equations (2), (3) for the rate of protein flow through the capillary wall are applied in the analysis. Here the diffusional flow is neglected for simplicity ($\Delta C = 0$). The mean protein concentration $\tilde{C}$ is defined as follows:

$$\tilde{C} = \begin{cases} C_v, J_v > 0, \\ C_i, J_v < 0. \end{cases} \tag{24}$$

The net balance of the inflow and outflow rates of fluid expresses the volume change of the intravascular and interstitial spaces. Let us separate the intravascular space into the plasma (p) and the red cell (rc) spaces for the convenience of discussing the colloid osmotic pressure of the blood, which is governed by the plasma volume and not by the intravascular space volume. Then the following equations can be written:

$$V_v = V_{rc} + V_p, \tag{25}$$

$$\frac{dV_{rc}}{dt} = Ht \cdot J, \tag{26}$$

$$\frac{dV_p}{dt} = -J_v + J(1 - Ht), \tag{27}$$

$$\frac{dV_i}{dt} = J_v. \tag{28}$$

The change in pressure caused by alteration of the volume in the intravascular or interstitial spaces has been analyzed by the Maxwell's visco-elastic law:

$$\frac{dP_v}{dt} = \frac{1}{c_v}\frac{dV_p}{dt} - \frac{1}{c_v \eta_v}\left(P_v - P_v^0\right), \tag{29}$$

$$\frac{dP_i}{dt} = \frac{1}{c_i}\frac{dV_i}{dt} - \frac{1}{c_i \eta_i}\left(P_i - P_i^0\right), \tag{30}$$

where c_v, c_i, η_v, η_i are the compliances and the viscosity coefficients of the intravascular and interstitial spaces, respectively, and P_v^0, P_i^0 are the stationary pressures of the spaces.

The colloid osmotic pressure is described by the Vant Hoff's equation:

$$\Pi = RT\frac{n}{V}, \tag{31}$$

where R is the gas constant, T is the absolute temperature and n is the quantity of a colloid osmotically active substance.

The variation of n for the intravascular fluid is given by a sum of protein flow through the capillary wall and the protein inflow:

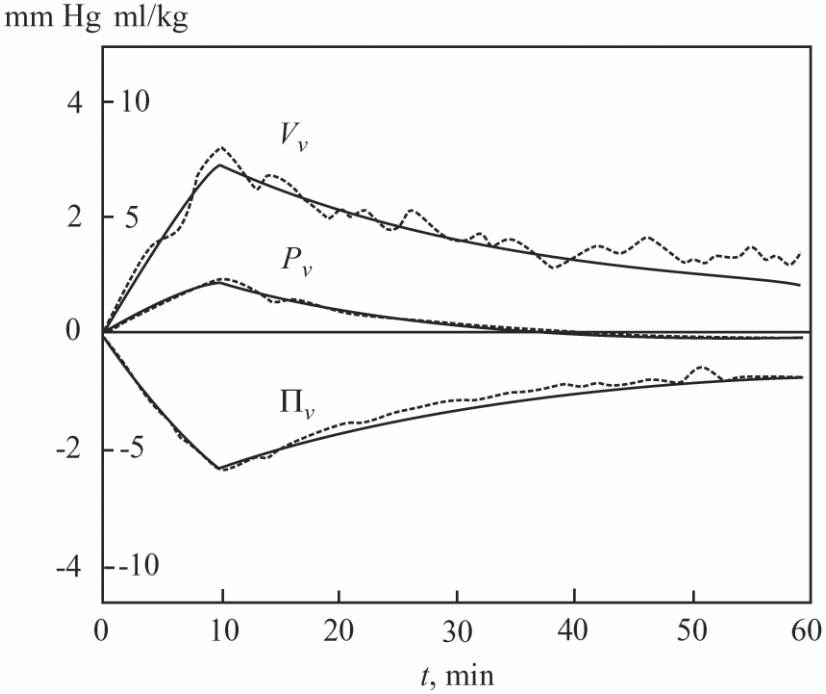

Fig. 5. The changes in blood volume (V_v), central venous pressure (P_v) and colloid osmotic pressure (Π_v) during saline infusion (the initial 10 min) and recovery (the following 50 min). Solid line – model data, dashed line – experimental data.

$$\frac{dn_v}{dt} = -J_s - J(1-Ht)\frac{\Pi_0}{RT}, \tag{32}$$

$$\frac{dn_i}{dt} = J_s, \tag{33}$$

where Π_0 is the colloid osmotic pressure of an inflow fluid. Substituting (32) and (33) into the expression of time derivative of the colloid osmotic pressure we get:

$$\frac{d\Pi_v}{dt} = -\frac{RT}{V_p}\left(J_s + J(1-Ht)\frac{\Pi_0}{RT}\right) - \frac{\Pi_v}{V_p}\frac{dV_p}{dt}, \tag{34}$$

$$\frac{d\Pi_v}{dt} = \frac{RT}{V_i}J_s - \frac{\Pi_i}{V_i}\frac{dV_i}{dt}. \tag{35}$$

Volume is represented in equation (34) not by V_v but by V_p, because the colloid osmotic pressure of blood is a function of the plasma volume and not the blood volume.

So there is a set of differential equations (2), (3), (24)-(30), (34), (35). Its solution gives us all variables as functions of time if the inflow rate J, the hematicrit Ht and the colloid osmotic pressure are given for the inflowing fluid.

The dependences of the volume, the hydrostatic pressure and the colloid osmotic pressure of the blood on time were compared with experimental data (Fig. 5). Results were in good agreement.

Jain et al. [7] present a mathematical model for transport of fluid and macromolecules in a tumor. A spherical uniformly perfused tumor embedded in normal tissue is under examination. A vessel in the tumor periphery is considered. According to the Starling's hypothesis, a quantity of plasma filters from the arterial end of a vessel into the interstitial space, and most of it is reabsorbed at the venous end. In normal tissue this residual fluid is reabsorbed by the lymphatics. In tumors, due to the absence of anatomically well-developed,

functioning lymphatics, the fluid leaked from a vessel can only go in two directions: towards the center of the tumor or towards the periphery. The inward flow would lead to an increase of the interstitial pressure. The outwardly flowing fluid would ooze into the surrounding normal tissue where it may be reabsorbed by the normal lymphatics. The velocity of this fluid in the interstitium u_i can be related to the interstitial pressure gradient by the Darcy law:

$$u_i = -k\frac{dP_i}{dr}, \tag{36}$$

where r is the radial position in the tumor, $k = \frac{K}{\eta}$.

Balancing the fluid filtered from the vessels with the fluid moving towards the tumor periphery yields the following equation of mass conservation:

$$\frac{1}{r^2}\frac{d\left(r^2 u_i\right)}{dr} = \frac{J_v}{V}, \tag{37}$$

where V is the tumor volume.

Substituting equations (36) and (37) into (1) leads to:

$$\frac{1}{r^2}\frac{d}{dr}\left(r^2\frac{dP_i}{dr}\right) = -\frac{L_p}{k}\frac{S}{V}\left[P_v - P_i - \sigma_T\left(\Pi_v - \Pi_i\right)\right]. \tag{38}$$

The boundary conditions are:

1 no fluid flux or pressure gradient at the center of the tumor;
2 continuous pressure and flow rate across the interface between the tumor and the surrounding normal tissue.

The outlet of the solute molecules from an exchange vessel and their following movement in the interstitium occurs by convection and diffusion. Mathematically the interstitial flux of macromolecules I_s is given by:

$$I_s = r_f u_i C_i - D\frac{dC_i}{dr}, \tag{39}$$

where D is the interstitial diffusion coefficient and r_f is the retardation factor (the ratio of the solute velocity to the fluid velocity). Balancing the solute leaving the vessel (3) with the solute moving in the interstitium (39) leads to the following convection-diffusion equation:

$$\frac{\partial C_i}{\partial t} = \frac{D}{r^2}\frac{\partial}{\partial r}\left(r^2\frac{\partial C_i}{\partial r}\right) - r_f\frac{1}{r^2}\frac{\partial}{\partial r}\left(r^2 u_i C_i\right) + \frac{J_s}{V}. \tag{40}$$

This equation was solved using the finite element method under the following boundary conditions:

1 the concentration and flux are continuous across the interface between the tumor and surrounding normal tissue;
2 there is no interstitial flux in the center of the tumor.

The solution gives $C_i = C_i(r,t)$ as a function of the radial coordinate and time after an injection.

Fig. 6 shows the comparison of the mathematical model with experimental data for a spherical tumor. High interstitial fluid pressure can be observed in tumors and it is supposed to be associated with the lack of functioning lymphatics, high vascular permeability and vascular collapse resulting from cells proliferation in a confined space. Analysis of model results allows authors to propose some ways to cure tumors [2, 3]. The results show a relatively high and uniform pressure in the center of the tumor and a sharp gradient of pressure in the periphery of the tumor. This leads to very little filtration of macromolecules from blood vessels in the center, as well as a convective flow in the tumor periphery, which

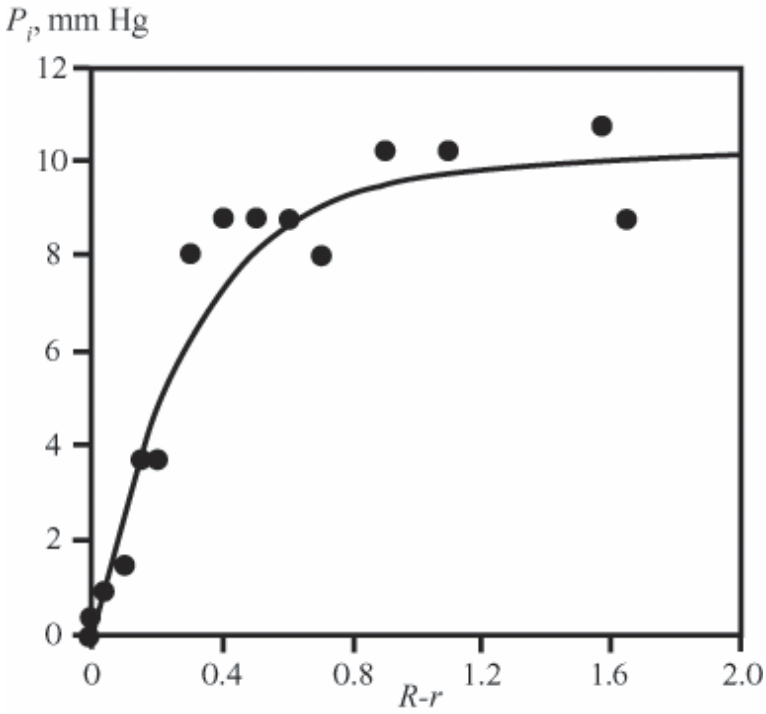

Fig. 6. Interstitial hydrostatic pressure in the tumor:
model data (solid line) and experimental data (circles).

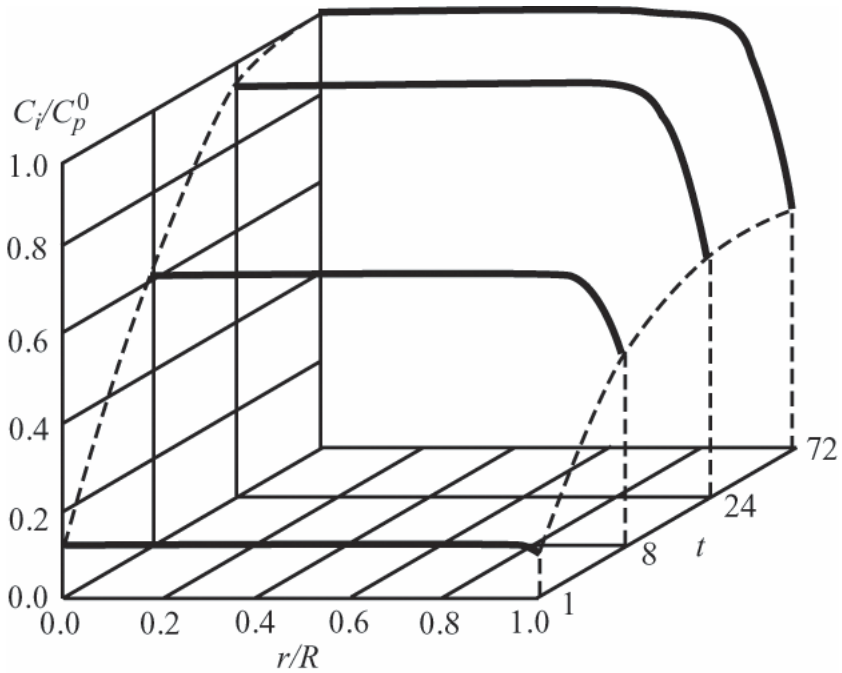

Fig. 7. Interstitial substance consentration in the tumor with a radius of 1 cm, during 72 h of continuous diffusion of this substance with concentration C_o^p.

tends to push the solute towards the edge of the tumor. Therefore the concentration of acting substances rapidly reaches a high value after a drug injection into the circulatory system while concentration at the periphery remains practically unchanged. To avoid the effect it was proposed either to increase filtration (by using vasoactive drugs) or to increase the diffusion component of the transcapillary flux because it helps to achieve a high drug concentration in the center of the tumor (Fig. 7).

A linear biphasic framework is used by Swartz et al. [18] to describe fluid movement between the interstitium and lymphatics. A constitutive equation for the tissue deformation as a response to an interstitial fluid injection is proposed in the following form:

$$\frac{\partial e}{\partial t} - K(2\mu + \lambda)\nabla^2 e + J_v = 0, \tag{41}$$

where e is the dilatation of the solid phase ($e = \nabla \cdot \boldsymbol{U}$; $\boldsymbol{U}$ is the average solid displacement vector), λ and μ are Lame's constants, J_v is the net fluid drainage. Although the lymphatics is primarily responsible for the fluid drainage following an interstitial injection, the term J_v must incorporate all mechanisms of fluid drainage including capillary reabsorption.

The simplest assumption for defining J_v is that drainage is linearly proportional to the interstitial fluid pressure:

$$J_v = \beta(P_i - P_b) = \beta P^*, \tag{42}$$

where β is the bulk effective conductance and P_b represents the baseline somatic fluid pressure. This pressure results from the various factors (including myogenic activity of the collecting lymphatic vessels, muscular movements, and respiratory oscillations), maintains the driving force for systemic lymph circulation and was considered constant (i.e. unaffected by the infusion).

The governing equation (41) can be expressed in terms of hydrostatic pressure:

$$\frac{1}{(2\mu + \lambda)}\frac{\partial P^*}{\partial x} - K\frac{\partial^2 P^*}{\partial x^2}\beta P^* = 0, \tag{43}$$

with the boundary and initial conditions:

$$P^*(0,t) = P_o^*,\ P^*(\infty,t) = 0, \tag{44}$$

where $P_o^* = (P_o - P_b)$ is the applied pressure.

The solution to Eq. (43) with the conditions (44) is:

$$P^*(x,t) = \frac{1}{2}e^{-x/\delta}\,erfc\left(\frac{x}{2\sqrt{K(2\mu+\lambda)t}} - \sqrt{\beta(2\mu+\lambda)t}\right) + \\ + \frac{1}{2}e^{x\delta}\,erfc\left(\frac{x}{2\sqrt{K(2\mu+\lambda)t}} + \sqrt{\beta(2\mu+\lambda)t}\right), \tag{45}$$

where $\delta = \sqrt{K/\beta}$ is the characteristic penetration length. The higher the ratio, the more the interstitial fluid movement dominates lymphatic drainage as a response to increased interstitial pressure.

By coupling experimental measurements with the theory the authors provide *in vivo* estimates of the tissue hydraulic conductivity, elastic modulus, and overall resistance to lymphatic drainage by measuring the response to the interstitial fluid injection under the constant pressure. It was also shown that the swelling associated with chronic lymphedema leads to an increase in hydraulic conductivity but not in lymphatic conductance; the decrease in lymphatic drainage seen with edema is rather due to a decrease in the driving force for drainage. The good agreement between the theory and experimental results, along with parameter estimations, which are within physiological ranges, supports the validity of the model and its assumptions. The model may serve as a foundation for studies of protein transport and drug delivery associated with lymphatic-based immune cells.

Integrated models

All models presented earlier consider only some aspects of microcirculation and extravascular fluid exchange. But since late 1990s there are attempts to describe the process as a whole. Such models depict coupled processes of the blood capillary flowing, the

transcapillary fluid and solute exchange and the interstitial fluid movement along with lymphatic drainage.

A complex model considering the circulation, a general interstitium, and the lymphatics, is formulated by Xie et al. [20] to describe the transport and distribution of fluid and plasma proteins (albumin) in the human microvascular exchange system. Transcapillary mass exchange is assumed to occur via a coupled Starling's mechanism. Unknown or poorly quantified model parameters are estimated by statistical fitting of simulation predictions to five different sets of experimental data.

Another model proposed by Kellen [10] describes the exchange of water and hydrophilic solutes among vascular, interstitial, and intercellular compartments of a cardiac tissue (Fig. 8). An important addition to the blood-tissue exchange region is another compartment representing the parenchymal cells. In cardiac tissue myocytes comprise a sizable fraction of the total tissue space, and can significantly change their volume during disturbances to the system. The system of partial differential equations describing solute and water exchange is:

$$
\begin{aligned}
&J_{vc} = L_{pc} S_c \left(\Delta P_c - RT \sum_{j=1}^{N} \sigma_T^j \Delta C^j \right), \\
&J_{vm} = L_{pm} S_m \left(\Delta P_m - RT \Delta C_m \right), \\
&J_{sc}^j = p^j S_c \Delta C^j \frac{Pe}{e^{Pe} - 1} + J_{vc} (1 - \sigma_T^j) \tilde{C}^j, \\
&P_c = (P_0 - P_L) \frac{L - x}{L} + P_L, \\
&\frac{\partial n_c^j}{\partial t} = -J_{sc}^j - \frac{\partial (u n_c^j)}{\partial x}, \\
&\frac{\partial n_i^j}{\partial t} = J_{sc}^j - K_L P_i C_i^j, \\
&\frac{\partial u}{\partial x} = \frac{A J_{vc}}{V_c S_c}, \\
&\frac{\partial V_i}{\partial t} = J_{vc} + J_{vm} - K_L P_i, \\
&\frac{\partial V_m}{\partial t} = -J_{vm}.
\end{aligned}
\qquad (46)
$$

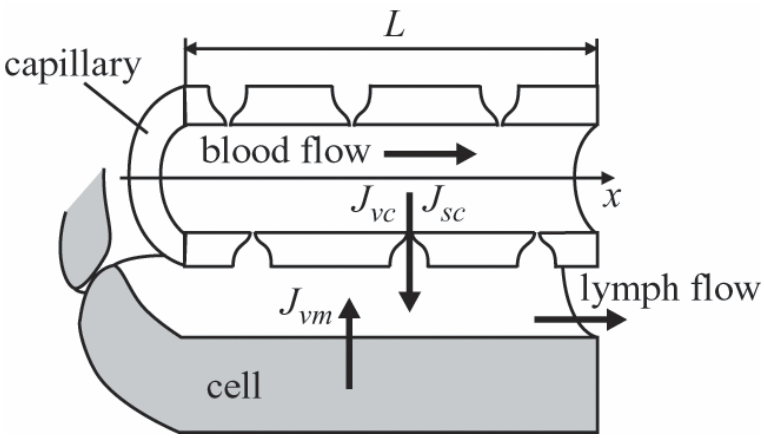

Fig. 8. The Kellen's model of microcirculatory substances transport.

Here lower indexes c, i and m denote values for the capillary, interstitium and cells (myocytes), respectively, and the upper index j denotes different solutes. The first three equations of (46) are Patlak's equations [14] describing flux of water and solutes from the capillary into the interstitium and from cells into the interstitium. The Patlak's model is the more correct than the model of Kedem and Katchalsky because it accurately accounts for the coupling of convective and diffusive fluxes across the membrane. The dimensionless Peclet's number $Pe = \frac{J_v(1-\sigma_T)}{pS}$ characterizes the ratio of convective to diffusive solute flux. The Kedem and Katchalsky solute flux equation is only valid for small Pe.

The next equation of the system gives the hydrostatic pressure distribution along the capillary. In the model, the assumption is made that changes in flow along the capillary length are minor, and the capillary pressure gradient is therefore linear and time invariant.

Finally the last equations give the change rate of solute moles in the capillary and in the interstitium and the change rate of volume for interstitial and cell spaces. The compliance of the capillary is supposed to be fairly small so its volume does not change. Besides, in this model, solute transport across the myocyte plasma membrane is not considered.

Lymphatic drainage of water and solutes is modeled as a distributed consumption term in the equation for the interstitium. The amount of interstitial fluid removed from the interstitium by the lymphatics is assumed to be proportional to the interstitial pressure, with a constant of proportionality K_L. It is also assumed that solute leaves the interstitium in amounts proportional to its concentration. This means that filtering across the lymphatic wall is negligible.

Conclusions

Experimental study of microscale exchange processes was started at the end of 19th century and models describing separate aspects of microcirculation are proposed for over 50 years but still there is no well-developed model of the whole process. This problem is complex, because it consists of the set of interdependent phenomena: blood flow in the capillary with extravascular fluid exchange, fluid movement in the tissue, exchange between tissue cells and interstitial fluid, fluid reabsorbsion into capillaries and lymphatics. Each of the set phenomena is not individually difficult to describe, but the interaction of many simple processes results in a fairly complex system. Nevertheless modeling of microcirculation and exchange process is a very important scientific and applied problem.

Acknowledgements

This work is partly funded by the Russian Fund of Basic Research (grants No. 01-01-00021 and No. 02-01-81026).

References

1. APELBLAT A., KATZIR-KATCHALSKY A., SILBERBERG A. A mathematical analysis of capillary-tissue fluid exchange. **Biorheology**, 11: 1-49, 1974.
2. BOUCHER Y., JAIN R.K. Microvascular pressure is the principal driving force for interstitial hypertension in solid tumors: implication for vascular collapse. **Cancer research**, 52: 5110-5114, 1992.
3. BOUCHER Y., JAIN R.K., BAXTER L.T. Interstitial pressure gradient in tissue-isolated and subcutaneous tumors: implication for therapy. **Cancer research**, 50: 4478-4484, 1990.
4. DAS B., BATRA R.L. Non-Newtonian flow of blood in an arteriosclerotic blood vessel with rigid permeable walls. **J theor Biol**, 175: 1-11, 1995.
5. HOGAN H.A., HENKIKSEN M. An evaluation of a micropolar model for blood flow through an idealized stenosis. **Journal of Biomechanics**, 22(3): 211-218, 1989.
6. ISOGAI Y., NOSE H., MIKI K., MORIMOTO T. Dynamics of fluid movement between intravascular and interstitial spaces. **J Theor Biol**, 100: 305-317, 1983.

7. JAIN R.K., BAXTER L.T. Mechanisms of heterogeneous distribution of monoclonal antibodies and other macromolecules in tumor: significance of elevated interstitial pressure. **Cancer Research**, 48: 7022-7032, 1988.
8. JONES I.P. Low Reynolds number flow past a porous spherical shell. **Proc Camb Phil Soc**, 73: 231-238, 1973.
9. KEDEM O., KATCHALSKY A. Thermodynamic analysis of the permeability of biological membranes to non-electrolytes. 1958 [classical article]. **Biochem Biophys Acta**: 413-30, 1989.
10. KELLEN M.R., BASSINGTHWAIGHTE J.B. Whole organ estimates of solute flux depend on flux partitioning among transcapillary exchange pathways. **Ann Biomed Eng**, 29: 15-73, 2001.
11. KROGH A.E., LANDIS E.M., TURNER A.H. The movement of fluid through the human capillary wall in relation to venous pressure and to the colloid osmotic pressure of the blood. **J Clin Invest**, 11: 63-95, 1932.
12. LANDIS E.M. Micro-injection studies of capillary permeability. II. The relation between capillary pressure and the rate at which fluid passes through the walls of single capillaries. **Am J Physiol**, 82: 528-542, 1927.
13. PAPPENHEIMER J.R.,. RENKIN E.M, BORRERO L.M. Filtration, diffusion, and molecular sieving through peripheral capillary membranes. **Am J Physiol**, 167: 13-46, 1951.
14. PATLAK C.S., GOLDSTEIN D.A., HOFFMAN J.F. The Flow of Solute and Solvent Across a Two-Membrane System. **J Theoretical Biology**, 5: 426-442, 1963.
15. ROHLF K., TENTI G. The role of the Womersley number in pulsatile blood flow: a theoretical study of the Casson model. **Journal of Biomechanics**, 34(1): 141-148, 2001.
16. SHIVAKUMAR P.N., NAGARAJ S., VEERABHADRAIAH R., RUDRAIAH N. Fluid movement in a channel of varying gap with permeable walls covered by porous medium. **Int J Enghg Sci**, 24(4): 479-492, 1986.
17. STARLING E.H. On the adsorbtion of fluid from interstitial spaces. **J Physiol**, 19: 312-326, 1896.
18. SWARTZ M.A., KAIPAINEN A., NETTI P.A., BREKKEN C., BOUCHER Y., GRODZINSKY A.J., JAIN R.K. Mechanics of interstitial-lymphatic fluid transport: theoretical foundation and experimental validation. **Journal of Biomechanics**, 32: 1297-1307, 1999.
19. VAJRAVELU K., SREENADH S., SAMAKRISHNA S., ARUNACHALAM P.V. Bingham fluid flow through a circular pipe with permeable wall. **Z angew Math Mech**, 67 (11): 568-569, 1987.
20. XIE S.L., REED R.K., BOWEN B.D., BERT J.L. A Model of Human Microvascular Exchange. **Microvascular Research**, 49(2): 141-162, 1995.
21. ZHANG J-B., KUANG Z-B. Study on blood constitutive parameters in different blood constitutive equations. **Journal of Biomechanics**, 33(3): 355-360, 2000.

МОДЕЛИ МИКРОЦИРКУЛЯЦИИ И ТРАНСКАПИЛЛЯРНОГО ОБМЕНА ЖИДКОСТЕЙ

Ю.И. Няшин, М.Ю.Няшин, Н.С. Шабрыкина (Пермь, Россия)

Доставка питательных веществ к органам и тканям, а также удаление продуктов обмена происходит в организме животных и человека с помощью кровеносной и лимфатической систем. Обменные процессы происходят на микроциркуляционном уровне и включают в себя следующие взаимосвязанные процессы: течение крови в капиллярах, транскапиллярный обмен, движение жидкости в интерстиции, обмен веществ между интерстициальной жидкостью и клетками ткани, дренаж в лимфатические капилляры. Основными движущими механизмами обмена веществ на микроуровне являются фильтрация и диффузия. Данная статья представляет собой обзор математических моделей описанных выше процессов. Библ. 21.

Ключевые слова: микроциркуляция, транскапиллярный обмен, математическое моделирование

Received 05 June 2002